Recent Advances in Positron Emission Tomography (PET) Imaging of Biomolecules: From Chemical Labeling to Cancer Diagnostics

Katsunori Tanaka* and Koichi Fukase

Department of Chemistry, Graduate School of Science, Osaka University, 1-1 Machikaneyama, Toyonaka, Osaka 560-0043, Japan

Abstract: The recent advances of PET using biomolecules, such as peptides, monoclonal antibodies, oligonucleotides, and glycoproteins will be described. So far, PET of biomolecules has been used mainly for diagnosis of cancers. The biomolecules have been conjugated with DOTA ligand, labeled with radiometals as the β^+ emitter, and targeted to specific tumors, where they have enabled visualization of even small metastatic lesions, due to the high sensitivity of the PET scanners.

Keywords: Positron emission tomography (PET), β^+ emitter, biomolecule, tumor, diagnosis, DOTA.

INTRODUCTION

Positron emission tomography (PET) is an emerging non-invasive method, which quantitatively visualizes the locations and the levels of radiotracer accumulation with a high imaging contrast [1]. While γ-camera-based scintigraphy such as SPECT (single-photon emission computerized tomography) is limited to a spatial resolution of 12-15 mm, the resolution of current clinical PET scanners is 4-6 mm. In addition, PET is about ten-times more sensitive than single-photon based methodologies, thus providing more accurate information on radiotracers accumulated at the low levels in tissues. In order to optimize PET tracers in small animal models in advance of clinical applications, the microPET technique has also been developed, and currently gives a volumetric resolution of $(1.8\ mm)^3$. The increasing availability and lower cost of PET scanners, together with the availability of radio- pharmaceuticals, make PET a routine technique for cancer diagnosis even in the clinical field, as well as an important tool in developing new molecular imaging probes that can target specific tissues and in elucidating unexplored biological pathways.

^{18}F-FDG (2-deoxy2-[^{18}F]fluoro-D-glucose, Fig. **1**) is a Food and Drug Administration (FDA)-approved radiopharmaceutical, and has become an important PET tracer in detecting primary and metastatic breast, lung and colorectal tumors, melanoma, and lymphoma, as well as monitoring responses to treatment, recurrence, and general prognosis. However, ^{18}F-FDG PET can often be confounded by benign disease as well as by active inflammation, which also exhibits elevated uptake of this tracer, leading to ambiguous conclusions. In order to circumvent such problem of ^{18}F-FDG, a variety of new small-molecule PET probes have been developed [2-5].

*Address correspondence to this author at the Department of Chemistry, Graduate School of Science, Osaka University, 1-1 Machikaneyama, Toyonaka, Osaka 560-0043, Japan; Tel: (+81) 6-6850-5391; Fax: (+81) 6-6850-5419; E-mail: ktzenori@chem.sci.osaka-u.ac.jp

Another interesting possibility for the cancer diagnosis is to use the biomolecules as the molecular imaging probes [1], since we can easily choose or design the desired peptides, proteins, antibodies, and oligonucleotides that exhibit high binding affinity to the target receptors, antigens, and nucleic acids being specifically overexpressed in or on tumor cells. Alternatively, the PET imaging of biomolecules can visualize their unknown *in vivo* kinetics where an important biological pathway is involved, which might lead to the discovery of the promising biomolecule-based drug candidates. So far, PET of biomolecules has mainly been used for diagnosis of cancers; therefore, in this review we would like to survey and focus primarily on these investigations. The best PET tracers for cancer diagnosis must show high and specific affinity to the target receptors which are overexpressed on the tumor cells. These compounds must also be efficiently internalized by tumor cells in order to achieve the tumor accumulation at high concentrations, as well as undergoing slow washout *in vivo*. Furthermore, tracers should be rapidly cleared from blood and exhibit low uptake in liver and kidney. Stability in the blood is also a very important factor for good tracers; on the other hand, a prolonged biological half-life places the patients in contact with radioactivity for a long time. PET experiments using biomolecules to target specific tumor tissues generally proceed as follows:

(1). The biomolecules, either synthesized, engineered, or isolated from natural sources, are labeled with radiometal ligands (see section 1). It is very important to attach ligands to biomolecules without inhibiting their activity. DOTA (1,4,7,10-tetraazacyclodecane-1,4,7,10-tetraacetic acid, Fig. **1**) is used as the most favorable ligand for biomolecular PET, due to its compatibility with a variety of radiometals, its extremely high stability [6-11], as well as the favorable clearance properties of the metal complexes *in vivo*, in comparison with other ligands [12,13]. This review only focuses on the DOTA ligand, which in our opinion is best suited for PET imaging purposes.

(2). DOTA-biomolecule conjugates are labeled with a variety of radiometals, and their binding affinity to target receptors, antigens, or complementary oligonucleotides are

1570-193X/08 $55.00+.00

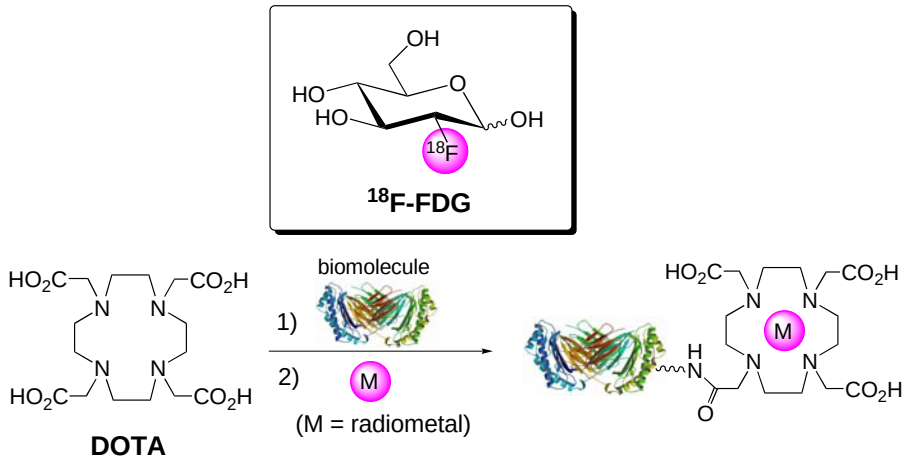

Fig. (1). ^{18}F-FDG and radiometal/DOTA as a biomolecule-based tracer.

first examined *in vitro*. Tumor cell internalization/exte-rnalization is also tested in cell-based assays. The typical radiometals cited in this review are summarized in Table **1**. Generally, radiometals with γ-emission are used for SPECT, while β^+ emitters can be used for PET diagnosis. On the other hand, β^- emitters can be specifically used for radiotherapeutic treatments. Since the radiometals introduced into the DOTA ligand show profound effects on the bioproperties of the tracers, the choice of radiometals is critical. Once a DOTA-biomolecule conjugate with a suitable radiometal has been determined *in vitro*, the same metal but with a different atomic weight can be directly used for PET imaging and radiotherapic treatments so that the properties of the tracers can be retained.

Table 1. Half Life and Applied Method of Radionuclides in this Review

Radiometals	Half Life ($t^{1/2}$)	Methods and Emitter Used in this Review	
^{66}Ga	9.5 h	PET	/β^+
^{67}Ga	78 h	SPECT	/γ
^{68}Ga	68 min	PET	/β^+
^{64}Cu	13 h	PET	/β^+
^{67}Cu	62 h	Radionuclide Therapy	/β^-
^{86}Y	15 h	PET	/β^+
^{90}Y	64 h	Radionuclide Therapy	/β^-
^{111}In	68 h	SPECT	/γ
^{18}F	110 min	PET	/β^+

(3). When suitable radiometal/DOTA-biomolecules have been determined, the tracers are examined for microPET imaging using small animal models, such as rats, implanted with tumor cells. The PET biodistribution data are compared with those obtained by other methods, such as SPECT (γ-scintigraphy imaging) and autoradiography, and the tracers are then evaluated for further optimizations. The same DOTA-bioconjugate can be used even for MR imaging (magnetic resonance) by incorporating paramagnetic metals, such as Gd^{3+}. Finally, the tracers with good properties can be subjected to clinical applications, namely, PET diagnosis and/or radionuclidic therapy for the patients.

The followings are recent and representative examples of biomolecule-based PET, mostly directed to cancer diagnosis.

1. LABELING METHODS OF BIOMOLECULES WITH DOTA LIGAND

Two methods have been widely used for the conjugation of DOTA or its derivatives to peptides, oligonucleotides, antibodies, and proteins (Scheme **1**, route 1 and 2). In one method, for the labeling of synthetic peptides, the commercially available tris-*t*-butyl-DOTA [14] is introduced during Fmoc-based solid-phase synthesis [Route 1 (i)]. The *t*-butyl protecting groups of DOTA and other acid-sensitive protecting groups are concomitantly removed at the end of peptide synthesis, followed by cleavage of peptides from the resin by treatment with neat TFA (trifluoroacetic acid) or TFA with scavengers. However, in some cases, *t*-butyl group deprotection is incomplete, or the DOTA/peptide conjugates decompose under the prolonged acid treatment. Recently, tris-allyl-DOTA was introduced and successfully applied to the DOTA/peptide synthesis [15]. The allyl groups in DOTA were quantitatively removed on the solid-phase by treatment with $Pd(PPh_3)_4$/morpholine in dichloromethane, followed by cleavage from the resin to provide the desired DOTA-labeled peptides at a purity sufficient for PET experiments. As more direct method, DOTA-labeled Fmoc-protected lysine has also been developed [Route 1, (ii)], and applied to the Fmoc-based solid-phase synthesis of DOTA-labeled peptides [14,16,17].

Secondly, especially for the labeling of proteins or antibodies, DOTA is introduced to the ε-amino group of lysine or the *N*-terminus of a protein by reaction with DOTA-*O*-succinimidyl ester (DOTA-OSu); the reaction is more favorable with DOTA-*O*-sulfosuccinimidyl ester (DOTA-OSSu), due to the better solubility of this compound in buffer solutions (Route 2). Thus, DOTA-OSSu prepared *in situ* from DOTA, EDC, and *N*-hydroxysulfosuccinimide (Sulfo-NHS), is directly reacted with the biomolecules, usually at room temperature overnight, to give the desired DOTA conjugates. This conventional method, using the

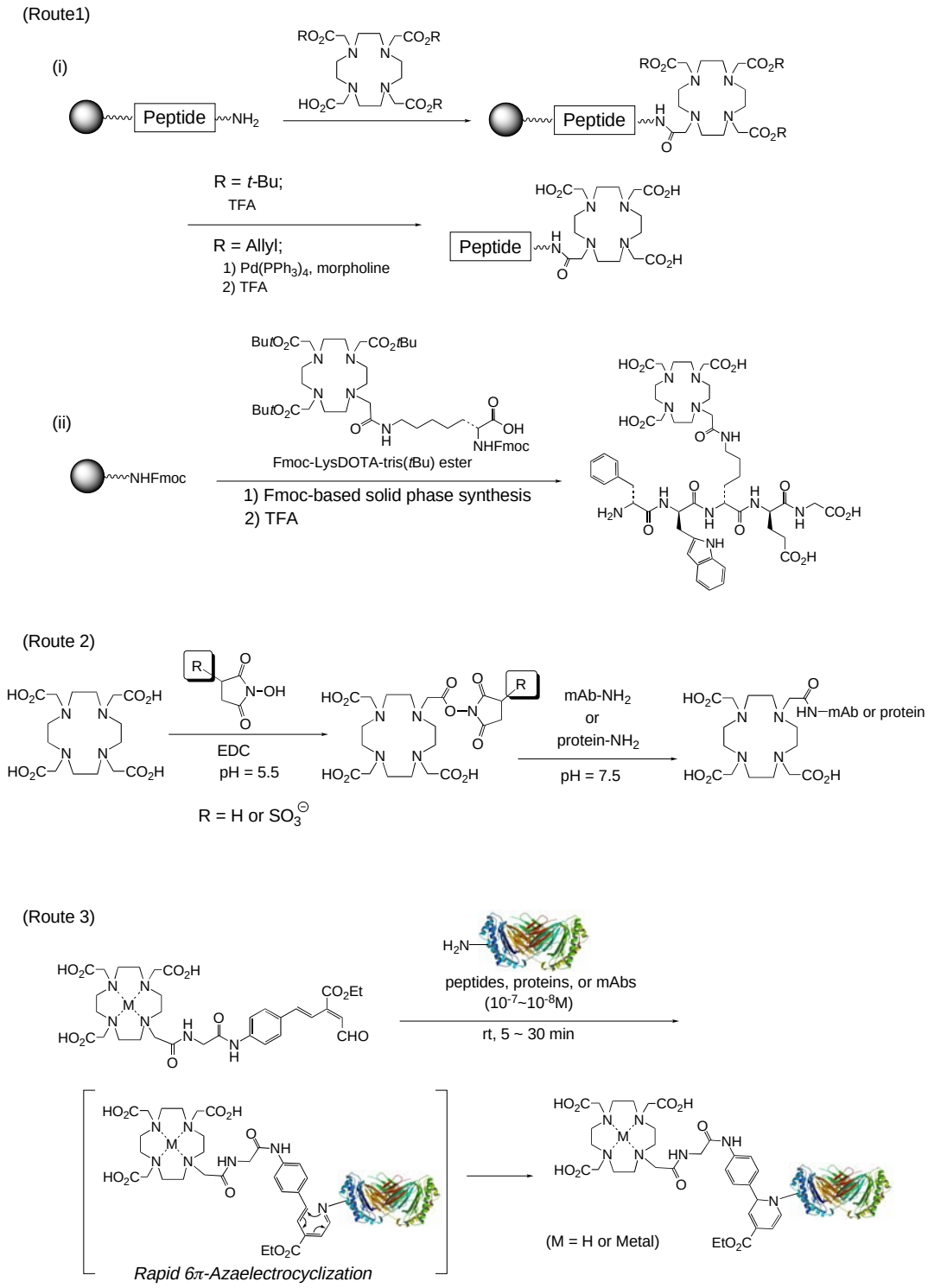

Scheme 1. Conjugation methods with biomolecules.

activated succinimidyl ester of DOTA, was further improved by optimizing the reaction conditions, both for preparation of the activated DOTA-OSSu and for conjugation to the antibody. The best conditions for conjugation to bio-molecules (in this case, antibody) involved incubation of the antibody with DOTA-OSSu in 0.1 M sodium phosphate buffer (pH = 7.5) at 4℃ for 24 h. By this method, the number of DOTA molecules introduced to the antibody were increased six-fold, while unfavorable antibody dimerization mediated by the active ester was significantly reduced [18]. This direct labeling method has also been used for conjugation with peptides and oligonucleotides, although the latter requires synthetically introduced amino linkers. The *p*-nitrophenyl ester or isothiocyanate derivatives of DOTA have also been used for this purpose [19,20].

Although the direct labeling of biomolecules by DOTA (such as using activated DOTA ester) is quite useful, the reactions usually proceed slowly and require as much as a few milligrams of sample in order to keep reaction concentrations high. Since PET experiments require only small amounts of tracers, and important biomolecules are sometimes obtained in only small amounts, a submicrogram-scale conjugation methodology would greatly expand the applicability of PET imaging. To address this issue, a submicrogram-scale labeling of lysine residues was developed *via* a rapid 6π-azaelectrocyclization (Route 3) [21]. One of the authors has discovered that unsaturated (*E*)-ester aldehyde derivatives quantitatively react with primary amines, including lysine, within 5 min in solution at a wide range of pH, providing 1,2-dihydropyridines as irreversible products [22-25]. This reaction proceeds *via* smooth azaelectrocyclization of the intermediary Schiff bases (1-azatrienes), which is strongly accelerated due to the efficient HOMO-LUMO interactions within the 1-azatriene systems and the presence of C4-electron withdrawing and C6-conjugated substituents [23]. Not only DOTA, but also other groups used in imaging (such as fluorescent groups), were efficiently and selectively introduced to lysines on a picomole scale, even at 10^{-7}~10^{-8} M concentrations of peptides, proteins, and monoclonal antibody, after an incubation of 5-30 min at room temperature. It is also noteworthy that the various metals, such as paramagnetic Gd^{3+}, can be chelated in the DOTA unit of the ester aldehyde probe, prior to the labeling of the peptide (Route 3). Therefore, this new process would allow for the efficient labeling of valuable and/or unstable materials.

2. PEPTIDE-BASED PET

Peptides are the most widely utilized tracers for the cancer diagnosis, since the peptides with the DOTA ligand introduced at the appropriate positions, are easily prepared by the solid-phase synthesis (Scheme **1**, Route 1) and the peptide structures can also be optimized from the combinatorial libraries. A variety of the peptide-based tracers which efficiently target the specific receptors on the tumor cells, has been examined. Recent and successful examples involve, i.e., the cyclic RGDyK derivatives as αVβ3-integrin agonists [26-30], the bombesin derivatives for the human gastrin-releasing peptide receptor (GRPR) [31-34], the α-melanocyte stimulating hormone analogs (α-MSH) for melanocortin type 1 receptor (MC1R) [35-37], and the peptidic human epidermal growth factor (hEGF) for epidermal growth factor receptor (EGFR) [38]. Here, the peptide-based diagnosis of the somatostatin receptor-expressing tumors is shown as a representative example.

Somatostatin-based PET imaging and radiotherapy is of great interest, since somatostatin receptors (SSTRs) are overexpressed in neuroendocrine tumors, i.e., gastroentero- pancreatic, small cell lung, breast, and sometimes tumors in the nervous systems [39]. Somatostatin is known to be easily degraded *in vivo*, and metabolically stable DOTA-octreotide derivatives have been developed. Out of many analogs prepared so far, [DOTA-DPhe^1,Tyr^3]-octreotide (DOTA-TOC, **1**, Fig. **2**) exhibited the highest affinity to the somatostatin receptor subtype 2 (SSTR2), which can be found in primary tumors as well as metastases; therefore, this probe has been useful for imaging of tumor-bearing mice, non-human primates, and human patients [40]. DOTA-TOC **1**, usually prepared by solid-phase synthesis (Scheme **1**, Route 1) was labeled with ^{111}In, ^{90}Y, and ^{67}Ga; binding affinity to SSTR2, internalization/externalization in the SSTR2-expressing AR4-2J pancreatic tumor cells, stability in serum, and biodistribution were studied in nude mice implanted with AR4-2J tumor cells [41,42]. ^{67}Ga-DOTA- TOC showed much higher SSTR2 affinity than the corresponding ^{111}In and ^{90}Y congeners and was found to be efficiently internalized by AR4-2J cells. Furthermore, ^{67}Ga- DOTA- TOC was rapidly removed from non-target organs including the kidney, resulting in excellent tumor-to-non- target tissues uptake ratios. The observed metal ion dependence was explained by the differences in the DOTA/metal-co-ordination structures, based on X-ray crystallographic analysis of simplified complex models. Ga^{3+} is hexa-coordinated by the four cyclen nitrogens and two carboxylates, while one carboxylate group and the amide oxygen are not involved in the metal co-ordination. This free carboxylate group may contribute to the efficient kidney clearance, while the structure of ^{67}Ga-DOTA-TOC, where the pharmacophoric peptide moiety was sufficiently separated enough by the free amide linker, resulted in improved receptor binding and hence high tumor uptake [41,42]. On the other hand, the octacoordinated structure of Y^{3+}/DOTA, in which the metal occupies all carboxylates, nitrogens, and amide linker groups, might induce congestion on the probe structure, leading to lower receptor binding affinity.

DOTA-TOC **1**, labeled with the positron-emitting radionuclide, ^{66}Ga ($t^{1/2}$ = 9.5 h), was investigated in AR4-2J-implanted mice by PET [43,44], and excellent tumor-to-organ ratios could be achieved due to its high receptor affinity. PET imaging of ^{86}Y congener ($t^{1/2}$ = 15 h) in non-human primates (baboons, *Papio hamadryas*) has been reported as well [45]. However, these two reports note relatively high uptake in kidney, which still remains to be improved.

The first PET of DOTA-TOC **1** in human patients was reported using gallium-68 ($t^{1/2}$ = 68 min) [46-50]. Meningiomas were selected as the target tumor because SSTR2 is overexpressed in these cancers. ^{68}Ga-DOTA-TOC was injected into patients suffering from meningiomas (tumor size of 7- to 25-mm diameter), and the results were compared with those obtained by SPECT (single-photon emission computerized tomography), MRI (magnetic resonance imaging), as well as ^{18}F-FDG PET. ^{68}Ga-DOTA-TOC was rapidly excreted from the blood, immediately accumulated in the meningiomas after the injection, and even the smallest tumors of 7- to 8-mm dia- meter could be clearly visualized. ^{68}Ga-DOTA-TOC tracer also detected the extent of meningiomas located beneath osseous structures, such as at the base of the skull. It is worthwhile mentioning that no radioactivity could be observed in normal brain tissues. On the other hand, SPECT and MRI have a sensitivity drawback in detecting small meningiomas, i.e., the methods failed in visualizing tumors at the base of the skull. Furthermore, the use of conventional ^{18}F-FDG PET tracer resulted in lower meningioma-to-background rations. Therefore, the ^{68}Ga-DOTA-TOC probe is very promising candidate not only as a

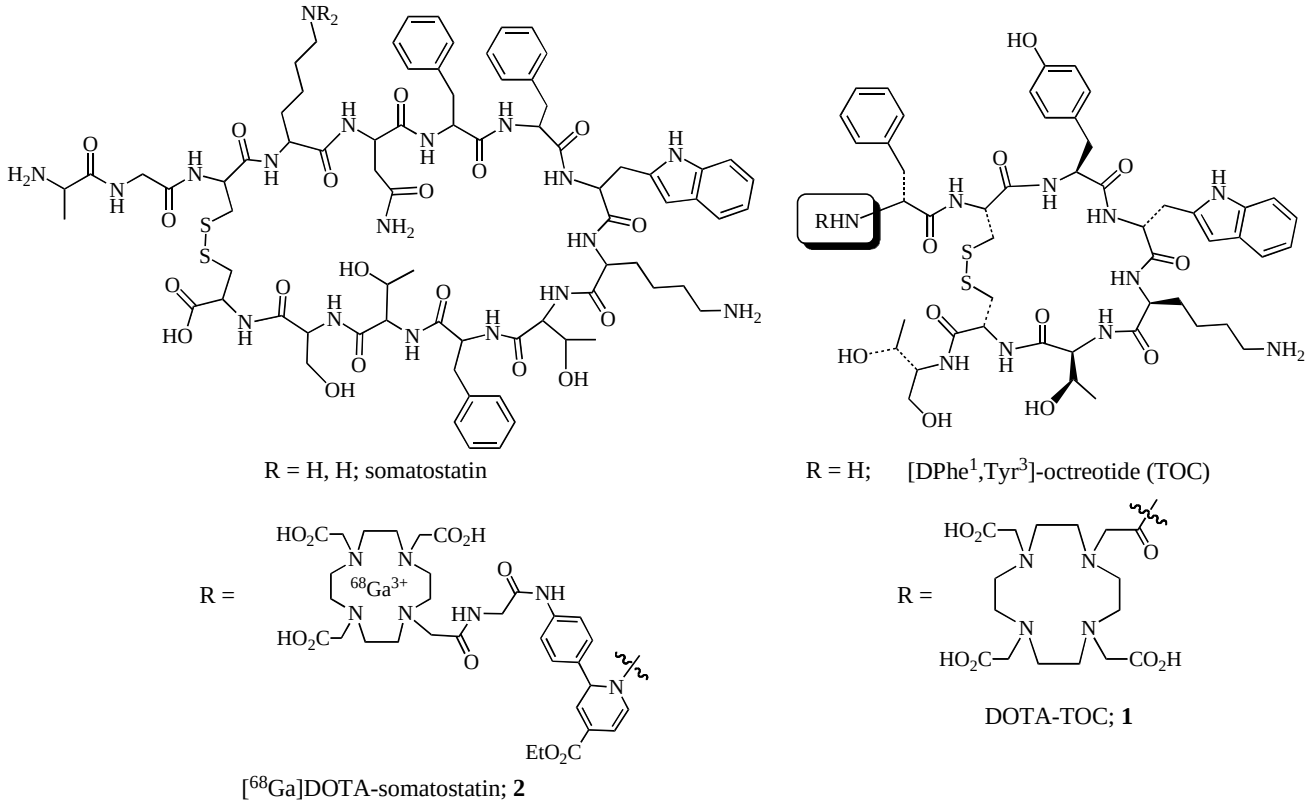

Fig. (2). Somatostatin and octreotide derivatives.

PET tracer of SSTR-positive tumors but also for radiotherapeutic applications, when suitable radiometals, such as ^{67}Ga, ^{90}Y, or even ^{67}Cu are used. DOTA-TOC **1** could be applied not only to PET, but also to diagnosis by SPECT of patients with differentiated thyroid cancer (DTC), which is difficult to accomplish by conventional measurements of serum thyroglobulin (Tg) levels and ^{131}I whole body scintigraphy (^{131}I-WBS) [51].

Finally, in order to circumvent the unfavorable kidney accumulation of the radiometal-DOTA-TOC tracer **1** during clinical treatments, amino acid co-infusion has been examined [52,53]. ^{86}Y-DOTA-TOC was administered to 24 patients with metastatic, non-resectable, neuroendocrine tumors, and the effects of co-infusion were monitored by PET. Renal uptake of ^{86}Y-DOTA-TOC could be reduced by infusion of a mixture of L-lysine and L-arginine, and more efficiently by the dipeptide Lys-Arg, without affecting tumor uptake. Although such a co-infusion of amino acids allows the patients to receive a higher dose of the tracers to be accumulated in the target tumors, the side effects of nausea and vomiting should be taken into consideration.

As described above, somatostatin itself was believed to be extremely unstable *in vivo* (stability in rat serum for just 5 min), and the previous imaging studies of somatostatin receptors were in all cases effected using a metabolically stable octreotide analogs. However, a recent study on microPET imaging of [^{68}Ga]DOTA-somatostatin **2** (Fig. **2**), prepared by a selective labeling of a single lysine that is not responsible for receptor binding (Scheme **1**, Route 3), successfully visualized the tracer accumulated in the pancreas of rabbit 2-4 h after injection (Fig. **3**) [21]. Given this new evidence of somatostatin stability in rabbit, as well as its clear accumulation in pancreas (somatostatin receptors are expressed on pancreas, kidney, as well as gastrointestinal tract) [39], this study might provide an intriguing oportunity to use somatostatin itself as a diagnostic tracer of endocrine tumors.

3. ANTIBODY-BASED PET DIAGNOSIS

The specific localization of radiometal-labeled antibodies to target tumors is a promising approach for PET diagnosis [54]. However, the use of whole antibodies suffers from their unfavorable properties *in vivo*, such as prolonged biological half-life and slow blood clearance, which result in low tumor-to-background ratios. On the other hand, the enzymatically generated antibody fragments, such as F(ab')$_2$ or Fab' (termed "minibodies"), show more favorable tumor targeting and clearance kinetics than the corresponding whole antibodies. In this section, a prominent example of minibody-based PET, a minibody of anti-HER2 protein antibody (herceptin) will be described. Furthermore, a concept of "pretargeted" immunodiagnosis using a whole antibody, will also be discussed.

HER2 (c-erbB2 or Her-2/neu) is a protooncogene, which encodes the 185-kDa transmembrane protein, human epidermal growth factor receptor 2 (HER2 protein). HER2 protein is overexpressed particularly in primary breast cancers as well as other malignancies, whereas it is expressed at low levels in normal tissues. Therefore, herceptin

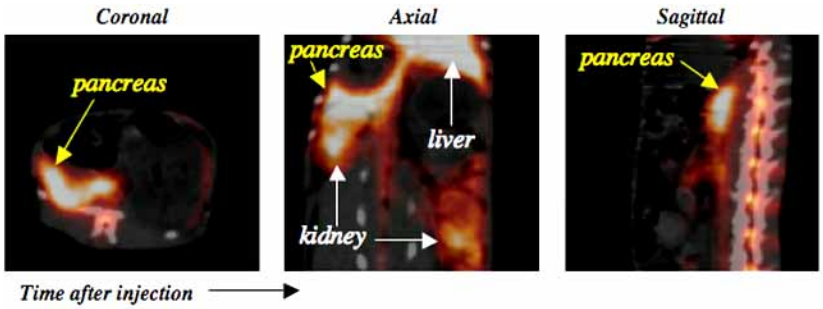

Fig. (3). PET imaging of [^{68}Ga]DOTA-somatostatin **2** in rabbit during 2-4 hours after injection (overlapped with CT).

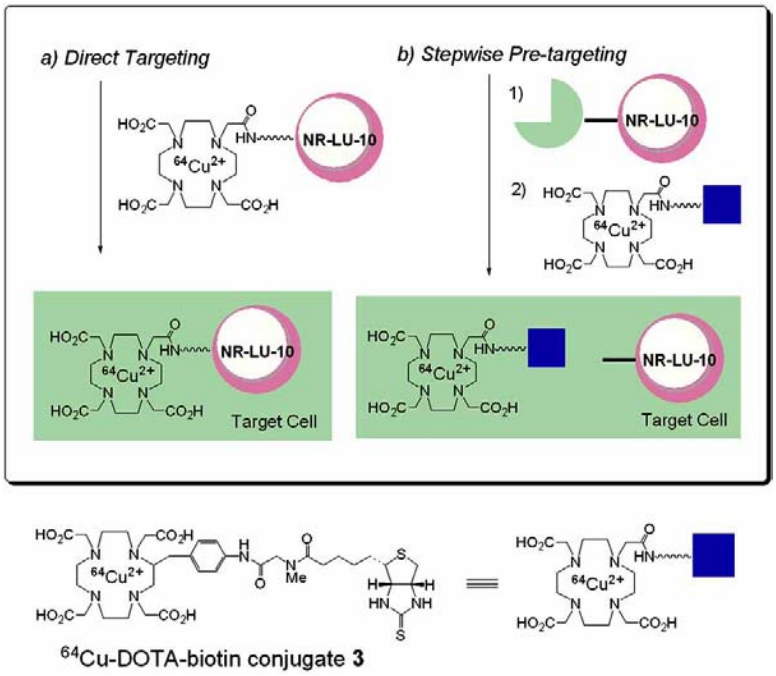

Fig. (4). "Pre-targeted" strategy of PET diagnosis.

(trastuzumab), a clinically applied anti-HER2 protein antibody, is a very attracting PET tracer for tumor imaging. Although herceptin itself shows good *in vivo* distribution and pharmacokinetics for PET study, the F(ab')$_2$ fragment of herceptin has a much shorter half-life, and is therefore suited for diagnostic purposes [55].

The F(ab')$_2$ fragment of herceptin, which was obtained by pepsin digestion of herceptin, was conjugated with DOTA by treatment with DOTA-OSu at pH 7.3 in water [56,57]. Characterization of the biodistribution, including microPET studies, were performed in mice bearing BT474 breast tumor xenografts, by using the ^{111}In- and ^{68}Ga-congeners, respectively. ^{111}In-DOTA-F(ab')$_2$-herceptin significantly accumulated in the HER2-overexpressed BT474 xenograft, whereas little accumulation was observed in MDA-MB-468 xenografts with high levels of EGFR expression (epidermal growth factor receptor); thus, the tracer achieved good tumor selectivity. Subsequently, microPET of ^{68}Ga-DOTA-F(ab')$_2$-herceptin in a mouse cancer model was also examined in response to treatment with a Hsp-90 inhibitor, 17-allylamino-17-demethoxygeldanamycin (17AAG). Hsp90 (heat shock protein 90) is a molecular chaperone which plays important roles in folding and stabilizing oncoproteins; PET of ^{68}Ga-DOTA-F(ab')$_2$-herceptin might follow the tumor expression and reduction, thus evaluating the drug pharmacodynamics of 17AAG. A significant decrease in HER2 protein was successfully visualized by this ^{68}Ga-tracer after treatment with 17AAG. In contrast, PET signals from the conventional ^{18}F-FDG tracer, which only measures the glycolysis inside the cells (an independent consequence of the HER2 downregulation), were unchanged.

Recently, a very interesting "pretargeted" PET strategy was reported in order to circumvent the unfavorable *in vivo* properties of a whole antibody, using anti-Ep-CAM antibody (NR-LU-10) in a xenograft-implanted mouse model of the human colorectal cancer, SW1222 (Fig. **4**) [58]. Cell adhesion molecules (CAM) are usually highly expressed in cancer cells, and therefore, anti-CAM antibody-based imaging, directed towards radioimmunotherapy (RIT), has actively been investigated. For this "pretargeted" protocol, a monoclonal antibody NR-LU-10 was first conjugated with streptavidin and injected to the xenograft-bearing mouse, prior to treatment with ^{64}Cu-DOTA-biotin **3** (thereby called as "pretargeted" strategy). The stability, clearance, biodistribution, and tumor targeting properties of ^{64}Cu-DOTA-biotin **3** in the "pretargeted" xenograft have been compared

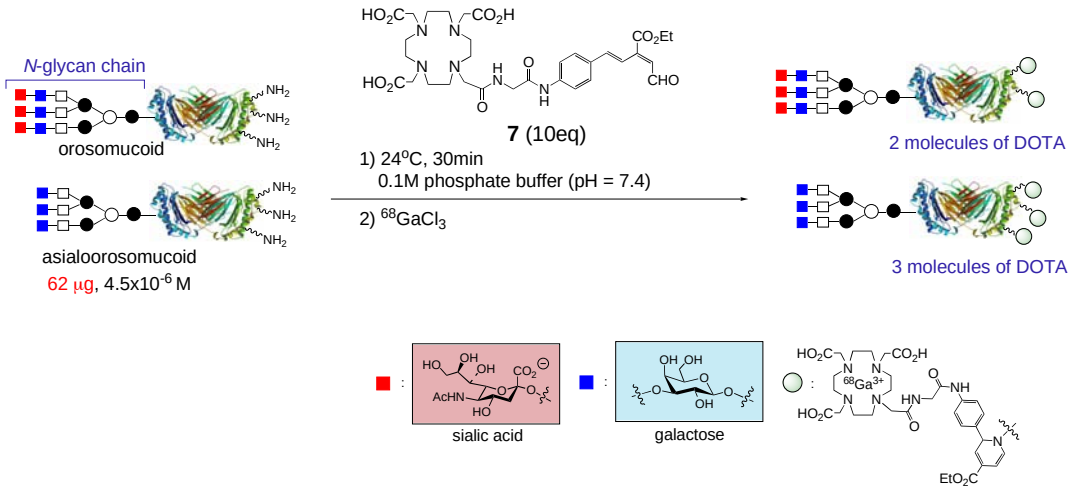

Scheme 2. Labeling of glycoproteins by DOTA.

with those of the conventional antibody-based PET targeting by ^{64}Cu-DOTA-NR-LU-10, which is prepared *via* direct labeling of the antibody with DOTA-OSSu. As expected, the small effector molecules of ^{64}Cu-DOTA-biotin **3** exhibited more rapid tumor uptake, substantially faster blood clearance and renal excretion, therefore resulting in superior tumor-to-normal tissues ratios. "Pretargeted" PET is thus a new and promising strategy for future antibody-based diagnosis [59,60].

4. MISCELLANEOUS (ALBUMINS, OLIGONUCLEOTIDES, AND OLIGOSACCHARIDES)

Serum Albumins as PET Blood-pool Markers

Since the growth of tumors depends on sufficient blood supply, radiolabeled serum albumins are useful for blood-pool imaging of angiogenic tumors, as well as for myocardial perfusion imaging. Both $H_2{}^{15}O$ and ^{68}Ga-DOTA-albumins (RSA; rat serum albumin), which was prepared by the method described in section 1 (Scheme **1**, Route 2), were applied to the mechanistic investigation of the inhibition of the malignant tumor growth by human angiotensin (hANG) [61]. hANG is one of the most potent inhibitors of endothelial cell proliferation, angiogenesis, and tumor growth *in vivo*. Changes in tumor perfusion and blood volume during the angiogenic process in the presence of overexpressed hANG were evaluated by PET, in ACI or RNU nude rats bearing subcutaneous MH3924A. MicroPET of these tracers showed that the tumor perfusion and blood volume were enhanced in hANG-overexpressed MH3924A compared with the wild-type MH3924A tumor, corresponding to both increased microvessel density and decreased necrosis. In a similar way, the tumor inhibition process by human tropinin I (TnI), another potent inhibitor of angiogenesis, has also been studied [62].

Oligonucleotides and Peptide Nucleic Acids (PNA) for Tumor Imaging

Antisense-based cancer PET imaging is a newly emerging area of noninvasive diagnosis technique. Since ras oncogene point mutations are found in a variety of human tumors but not in normal tissues (e.g., they are expressed with extremely high ratio in pancreatic carcinomas), the ras messenger RNA (mRNA) is an attractive target for gene-based diagnosis. 17-mer oligonucleotides consisting of a base sequence of 5'-CTACGCCACTAGCTCCA-3' with three metabolically stable backbones, namely, 2'-deoxyphos phodiester (PO, **4**), 2'-deoxyphosphorothioate (PS, **5**), and 2'-*O*-methyl phosphodiester (OMe, **6**) have been designed to target the codon 12 point mutation of human K-ras oncogene (Fig. **5**) [63,64]. After labeling by ^{64}Cu-DOTA at the 5'-aminohexyl moiety of the oligonucleotides *via* the DOTA-OSSu method, their biokinetics, biodistribution, as well as microPET were examined in athymic rats, bearing either a tumor of A549 cells with K-ras point mutation in codon 12, or a tumor of BxPC-3 cells with wild-type K-rasA [65].

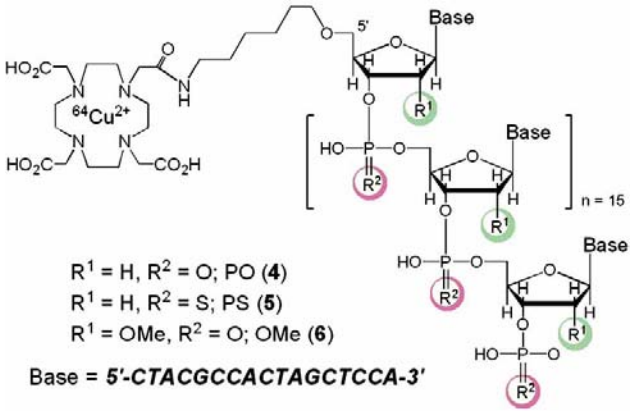

Fig. (5). ^{64}Cu-DOTA-oligonucleotide-based PET tracers.

Better localization images were obtained from microPET of A549 cells when using PS **5** and OMe **6** than when using PO **4**, while a slightly better uptake of PS **5** was observed in A549 cells than in BxPC-3 cells with wild-type K-rasA. However, the nuclease-mediated rapid degradation of OMe **6** and the low tumor selectivity as well as non-specific accumulation of PS **5** in the kidney require further improvements of these tracers: metabolic stability, hybridization ability, cell permeability, and binding specificity must all be addressed. In addition, the effects of the oligonucleotide length on

biodistribution should be investigated in detail for future applications. In order to circumvent the metabolic instability of the oligonucleotides, the application of peptide nucleic acid (PNA) congeners to gene-based PET has also been reported [66].

Visualization of Sialic Acid-dependent Circulatory Residence of Glycoptoteins by PET

Although FDG is widely used as a monosaccharide PET tracer for cancer diagnosis, PET of oligosaccharides and glycoproteins is a totally unexplored field. Very recently, a first microPET of glycoproteins, orosomucoid and asialo-orosomucoid was reported in order to investigate the effects of *N*- and/or *O*-glycans on the metabolic stability of the proteins [21]. Based on the smooth electrocyclization protocol (Scheme **1**, Route 3), glycoproteins available in only small amounts (62 μg of orosomucoid and asialo-orosomucoid) were labeled successfully with the incorporation of ~2-3 units of DOTA by incubating the respective protein with 10 equivalents of aldehyde probe **7** for 30 min, followed by purification by quick size-partitioning gel-filtration (Scheme **2**). The DOTA-labeled glycoproteins were subsequently radiometallated with ^{68}Ga and their *in vivo* kinetics were analyzed in rabbit by means of PET. [^{68}Ga]DOTA-orosomucoid and asialoorosomucoid adducts successfully visualized the asialo-glycoprotein being cleared through kidney faster than the orosomucoid (Fig. **6**), thus achieving the first visualization of sialic acid-dependent circulatory residence of glycoproteins. The results are in good agreement with well-known hypotheses of the clearance of the proteins through the asialoglycoprotein receptor in the liver [67]: namely, the sialic acid residue on the non-reducing end of the oligosaccharides contributes to the stability of glycoproteins in the blood, while the sialidase-mediated production of asialoglycoproteins, bearing the galactose residue at the non-reducing end of the oligosaccharides, is responsible for the metabolic pathway. These promising PET images of glycoproteins suggest future uses for these glycoproteins in pharmacological and/or clinical applications.

5. FUTURE PROSPECTIVE

As is clear from the selected examples cited in this review, PET imaging of biomolecules has recently become one of the most promising strategies for tumor diagnosis, due to the close collaborations between chemists, biologists, and physicians. From a chemistry point of view, if the labeled biomolecules could be more easily accessed, one could more rapidly discover favorable PET tracers, thus greatly expanding the biomolecule-based PET strategy. Although PET experiments require only a few nanograms to micrograms of the tracers, under the current labeling protocols, the engineered mAbs must be used as much as 5-20 mg. Once more rapid and efficient labeling chemistry is developed, we can find a new way to utilize unstable, important, and precious materials for diagnosis. Once promising candidates for peptide- or oligosaccharide-based tracers are determined, modular approaches to the chemistry will facilitate the optimization of the best tracer from combinatorial libraries.

The investigation of dual detection probes, e.g., probes that are detectable both by PET and fluorescence, will also become more important. A new molecular imaging probe has now been developed by taking advantage of the unique energy transfer of the lantanide/DOTA complexes, which has led to the emerging field of fluorescence (either utilizing Tb or Eu) and NIR (Near Infrared, by metalation with Yb or Er) techniques [68,69]. Such a new design of the probes will greatly facilitate biomolecule-based PET, where the stability of the tracers can be simultaneously detected by HPLC.

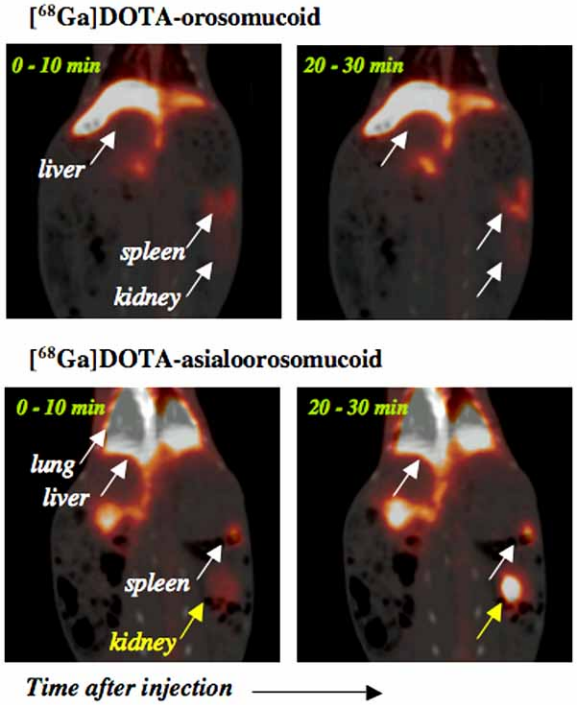

Fig. (6). MicroPET images of [^{68}Ga]DOTA-glycoproteins in rabbits (overlapped with CT). Time course of accumulation of [^{68}Ga]DOTA-orosomucoid and [^{68}Ga]DOTA-asialoorosomucoid in some peripheral organs (axial views).

Followed by peptides, antibodies, proteins and oligonucleotides as mainly described in this review, the authors strongly believe that oligosaccharide-based tracers are the next candidates to be developed. Surprisingly, to the best of our knowledge, oligosaccharide-based PET has not been reported, except in the case of the ^{18}F-FDG tracer (technically a monosaccharide) and very limited examples of glycoproteins, as described in Fig. (**6**). This is due to the difficulty in obtaining the structurally pure oligosaccharides from nature, and also because synthetic methods for complex oligosaccharides are still under development compared with the peptide synthesis, i.e., by automated solid-phase synthesis. In addition, the biological activity of the oligosaccharides is closely related to their heterogeneous environment, i.e., on the proteins (*O*- or *N*-linked glycans) and on the cell surfaces (such as ceramides), which are usually composed of clusters of mixed oligosaccharides. When such complex and structurally pure oligosaccharide molecules are easily accessible by chemical synthesis, and when the heterogeneous environment of oligosaccharides can be mimicked, it may be possible to target either tumors or inflammation

more efficiently than by peptide- or the antibody-based tracers.

ACKNOWLEDGMENTS

We acknowledge Professor Yasuyoshi Watanabe and Dr. Hiroshi Mizuma at RIKEN, Japan for helpful discussion in preparing the manuscript. Parts of the work cited in this review were financially supported by Grants-in-Aid for Scientific Research No. 19681024 and 19651095 from the Japan Society for the Promotion of Science, Collaborative Development of Innovative Seeds from Japan Science and Technology Agency (JST), New Enegry and Industrial Technology Development Organization (NEDO, project ID: 07A01014a), Research Grants from Yamada Science Foundation, as well as Molecular Imaging Research Program, Grants-in-Aid for Scientific Research from Ministry of Education, Culture, Sports, Science and Technology (MEXT).

REFERENCES

[1] Gambhir, S.S. *Nat. Rev. Cancer*, **2002**, *2*, 683.
[2] Suzuki, M.; Doi, H.; Bjorkman, M.; Anderson, Y.; Langstorm, B.; Watanabe, Y.; Noyori, R. *Chem. Eur. J.*, **1997**, *3*, 2039.
[3] Suzuki, M.; Noyori, R.; Langstom, B.; Watanabe, Y. *Bull. Chem. Soc. Jpn.*, **2000**, *73*, 1053.
[4] Suzuki, M.; Doi, H.; Hosoya, T.; Langstom, B.; Watanabe, Y. *Trends Anal. Chem.*, **2004**, *23*, 595.
[5] Hosoya, T.; Sumi, K.; Doi, H.; Wakao, M.; Suzuki, M. *Org. Biomol. Chem.*, **2006**, *4*, 410.
[6] Loncin, M. F.; Desreux, J. F.; Merciny, E. *Inorg. Chem.*, **1986**, *25*, 2646.
[7] Cacheris, W. P.; Nickle, S. K.; Sherry, A. D. *Inorg. Chem.*, **1987**, *26*, 958.
[8] Kumar, K.; Magerstadt, M.; Gansow, O. A. *J. Chem. Soc., Chem. Commun.*, **1989**, 145.
[9] Broan, C. J.; Cox, J. P. L.; Craig, A. S.; Kataky, R.; Parker, D.; Harrison, A.; Randall, A. M.; Ferguson, G. *J. Chem. Soc., Perkin Trans.*, **1991**, *2*, 87.
[10] Clarke, E. T.; Martell, A. T. *Inorg. Chim. Acta*, **1991**, *190*, 27.
[11] Clarke, E. T.; Martell, A. T. *Inorg. Chim. Acta*, **1991**, *190*, 37.
[12] Byegard, J.; Skarnemark, G.; Skalberg, M. *J. Radioanal. Nucl. Chem.*, **1999**, *241*, 281.
[13] Maecke, H. R. *Radiolabeled Peptides in Nuclear Oncology: Influence of Peptide Structure and Labeling Strategy on Pharmacology*. Springer., **2005**, 43.
[14] Available from Macrocyclics: http://www.macrocyclics.com/.
[15] Wangler, B.; Beck, C.; Wagner-Utermann, U.; Schirrmacher, E.; Bader, C.; Rosch, F.; Schirrmacher, R.; Eiseuhut, M. *Tetrahedron Lett.*, **2006**, *47*, 5985.
[16] De Leon-Rodriguez, L. M.; Kovacs, Z.; Dieckmann, G. R.; Sherry, A. D. *Chem. Eur. J.*, **2004**, *10*, 1149.
[17] Lewis, M. R.; Jia, F.; Gallazzi, F.; Wang, Y.; Zhang, J.; Shenoy, N.; Lever, S. Z.; Hannink, M. *Bioconjug. Chem.*, **2002**, *13*, 1176.
[18] Lewis, M. R.; Kao, J. Y.; Anderson, A.-L. J.; Shively, J. E.; Raubitschek, A. *Bioconjug. Chem.*, **2001**, *12*, 320.
[19] Peterson, J. J.; Pak, R. H.; Meares, C. F. *Bioconjug. Chem.*, **1999**, *10*, 316.
[20] Yoo, B.; Pagel, M. D. *Tetrahedron Lett.*, **2006**, *47*, 7327.
[21] Tanaka, K.; Masuyama, T.; Hasegawa, K.; Tahara, T.; Mizuma, H.; Wada, Y.; Watanabe, Y.; Fukase, K. *Angew. Chem. Int. Ed.*, **2008**, *47*, 102.
[22] Tanaka, K.; Kamatani, M.; Mori, H.; Fujii, S.; Ikeda, K.; Hisada, M.; Itagaki, Y.; Katsumura, S. *Tetrahedron*, **1999**, *55*, 1657.
[23] Tanaka, K.; Mori, H.; Yamamoto, M.; Katsumura, S. *J. Org. Chem.*, **2001**, *66*, 3099.
[24] Tanaka, K.; Katsumura, S. *J. Am. Chem. Soc.*, **2002**, *124*, 9660.
[25] Tanaka, K.; Kobayashi, T.; Mori, H.; Katsumura, S. *J. Org. Chem.*, **2004**, *69*, 5906.
[26] Chen, X.; Park, R.; Tohme, M.; Shahinian, A. H.; Bading, J. R.; Conti, P. S. *Bioconjug. Chem.*, **2004**, *15*, 41.
[27] Chen, X.; Liu, S.; Hou, Y.; Tohme, M.; Park, R.; Bading, J. R.; Conti, P. S. *Mol. Imag. Biol.*, **2004**, *6*, 350.
[28] Chen, X.; Hou, Y.; Tohme, M.; Park, R.; Khankaldyyan, V.; Gonzales-Gomez, I.; Bading, J. R.; Laug, W. E.; Conti, P. S. *J. Nucl. Med.*, **2004**, *45*, 1776.
[29] Chen, X.; Sievers, E.; Hou, Y.; Park, R.; Tohme, M.; Bart, R.; Bremner, R.; Bading, J. R.; Conti, P. S. *Neoplasia*, **2005**, *7*, 271.
[30] Wu, Y.; Zhang, X.; Xiong, Z.; Cheng, Z.; Fisher, D. R.; Liu, S.; Gambhir, S. S.; Chen, X. *J. Nucl. Med.*, **2005**, *46*, 1707.
[31] Chen, X.; Park, R.; Hou, Y.; Tohme, M.; Shahinian, A. H.; Bading, J. R.; Conti, P. S. *J. Nucl. Med.*, **2004**, *45*, 1390.
[32] Rogers, B. E.; Bigott, H. M.; McCarthy, D. W.; Manna, D. D.; Kim, J.; Sharp, T. L.; Welch, M. J. *Bioconjug. Chem.*, **2003**, *14*, 756.
[33] Yang, Y.-S.; Zhang, X.; Xiong, Z.; Chen, X. *Nucl. Med. Biol.*, **2006**, *33*, 371.
[34] Schuhmacher, J.; Zhang, H.; Doll, J.; Macke, H. R.; Matys, R.; Hauser, H.; Henze, M.; Haberkorn, U.; Eisenhut, M. *J. Nucl. Med.*, **2005**, *46*, 691.
[35] Froidevaux, S.; Calame-Christe, M.; Schuhmacher, J.; Tanner, H.; Saffrich, R.; Henze, M.; Eberle, A. N. *J. Nucl. Med.*, **2004**, *45*, 116.
[36] McQuade, P.; Miao, Y.; Yoo, J.; Quinn, T. P.; Welch, M. J.; Lewis, J. S. *J. Med. Chem.*, **2005**, *48*, 2985.
[37] Giblin, M. F.; Wang, N.; Hoffman, T. J.; Jurissson, S. S.; Quinn, T. P. *Proc. Natl. Acad. Sci. USA*, **1998**, *95*, 12814.
[38] Velikyan, I.; Sundberg, A. L.; Lindhe, O.; Hoglund, A. U.; Eriksson, O.; Werner, E.; Carlsson, J.; Bergstrom, M.; Langstrom, B.; Tolmachev, V. *J. Nucl. Med.*, **2005**, *46*, 1881.
[39] Maecke, H. R.; Hofmann, M.; Haberkorn, U. *J. Nucl. Med.*, **2005**, *46*, 172S.
[40] Froidevaux, S.; Eberle, A. N. *Biopolymers*, **2002**, *66*, 161.
[41] Heppeler, A.; Froidevaux, S.; Macke, H. R.; Jermann, E.; Behe, M.; Powell, P.; Hennig, M. *Chem. Eur. J.*, **1999**, *5*, 1974.
[42] Froidevaux, S.; Eberle, A. N.; Christe, M.; Sumanovski, L.; Heppeler, A.; Schmitt, J. S.; Eisemwiener, K.; Beglinger, C.; Macke, H. R. *Int. J. Cancer*, **2002**, *98*, 930.
[43] Ugur, O.; Kothari, P. J.; Finn, R. D.; Zanzonico, P.; Ruan, S.; Guenther, I.; Maecke, H. R.; Larson, S. M. *Nucl. Med. Biol.*, **2002**, *29*, 147.
[44] Lewis, M. R.; Reichert, D. E.; Laforest, R.; Margenau, W. H.; Shefer, R. E.; Klinkowstein, R. E.; Hughey, B. J.; Welch, M. J. *Nucl. Med. Biol.*, **2002**, *29*, 701.
[45] Rosch, F.; Herzog, H.; Stolz, B.; Brockmann, J.; Kohle, M.; Muhlensiepen, H.; Marbach, P.; Muller-Gartner, H.-W. *Eur. J. Nucl. Med.*, **1999**, *26*, 358.
[46] Henze, M.; Schuhmacher, J.; Hipp, P.; Kowalski, J.; Becker, D. W.; Doll, J.; Macke, H. R.; Hofmann, M.; Debus, J.; Haberkorn, U. *J. Nucl. Med.*, **2001**, *42*, 1053.
[47] Henze, M.; Dimitrakopoulou-Strauss, A.; Milker-Zabel, S.; Schuhmacher, J.; Strauss, L. G.; Doll, J.; Macke, H. R.; Eisenhut, M.; Debus, J.; Haberkorn, U. *J. Nucl. Med.*, **2005**, *46*, 763.
[48] Milker-Zabel, S.; Bois, A. Z.-D.; Henze, M.; Huber, P.; Schulz-Ertner, D.; Hoess, A.; Haberkorn, U.; Debus, J. *Int. J. Radiat. Oncol. Biol. Phys.*, **2006**, *65*, 222.
[49] Meyer, G.-J.; Macke, H.; Schuhmacher, J.; Knapp, W. H.; Hofmann, M. *Eur. J. Nucl. Med. Mol. Imaging*, **2004**, *31*, 1097.
[50] Breeman, W. A. P.; de Jong, M.; de Blois, E.; Bernard, B. F.; Konijnenberg, M.; Krenning, E. P. *Eur. J. Nucl. Med. Mol. Imaging*, **2005**, *32*, 478.
[51] Rodrigues, M.; Traub-Weidinger, T.; Leimer, M.; Li, S.; Andreae, F.; Angelberger, P.; Dudczak, R.; Virgolini, I. *Eur. J. Nucl. Med. Mol. Imaging*, **2005**, *32*, 1144.
[52] Jamer, F.; Barone, R.; Mathieu, I.; Walrand, S.; Laber, D.; Carlier, P.; de Camps, J.; Schran, H.; Chen, T.; Smith, M. C.; Bouterfa, H.; Valkema, R.; Krenning, E. P.; Kvols, L. K.; Pauwels, S. *Eur. J. Nucl. Med. Mol. Imaging*, **2003**, *30*, 510.
[53] Barone, R.; Pauwels, S.; Camps, J. D.; Krenning, E. P.; Kvols, L. K.; Smith, M. C.; Bouterfa, H.; Devuyst, O.; Jamer, F. *Nephrol. Dial. Transplant.*, **2004**, *19*, 2275.
[54] Schubiger, P. A.; Alberto, R.; Smith, A. *Bioconjug. Chem.*, **1996**, *7*, 165.
[55] Olafsen, T.; Kenanova, V. E.; Sundaresan, G.; Anderson, A.-L.; Crow, D.; Yazaki, P. J.; Li, L.; Press, M. F.; Gambhir, S. S.; Wiliams, L. E.; Wong, J. Y. C.; Raubitschek, A. A.; Shively, J. E.; Wu, A. M. *Cancer Res.*, **2005**, *65*, 5907.

[56] Smith-Jones, P. M.; Solit, D.; Afroze, F.; Rosen, N.; Larson, S. M. *J. Nucl. Med.*, **2006**, *47*, 793.
[57] Smith-Jones, P. M.; Solit, D. B.; Akhurst, T.; Afroze, F.; Rosen, N.; Larson, S. M. *Nat. Biotechnol.*, **2004**, *22*, 701.
[58] Lewis, M. R.; Wang, M.; Axworthy, D. B.; Theodore, L. J.; Mallet, R. W.; Fritzberg, A. R.; Welch, M. J.; Anderson, C. J. *J. Nucl. Med.*, **2003**, *44*, 1284.
[59] Axworthy, D. B.; Reno, J. M.; Hylarides, M. D.; Mallet, R. W.; Theodore, L. J.; Gustavson, L. M.; Su, F.-M.; Hobson, L. J.; Beaumier, P. L.; Fritzberg, A. R. *Proc. Natl. Acad. Sci. USA*, **2000**, *97*, 1802.
[60] Forster, G. J.; Santos, E. B.; Smith-Jones, P. M.; Zanzonico, P.; Larson, S. M. *J. Nucl. Med.*, **2006**, *47*, 140.
[61] Schmidt, K.; Hoffend, J.; Altmann, A.; Strauss, L. G.; Dimitrakopoulou-Strauss, A.; Engelhardt, B.; Koczan, D.; Peter, J.; Dengler, T. J.; Mier, W.; Eisenhut, M.; Haberkorn, U.; Kinscherf, R. *J. Nucl. Med.*, **2006**, *47*, 543.
[62] Schmidt, K.; Hoffend, J.; Altmann, A.; Kiessling, F.; Strauss, L. G.; Koczan, D.; Mier, W.; Eisenhut, M.; Kinscherf, R.; Haberkorn, U. *J. Nucl. Med.*, **2006**, *47*, 1506.
[63] Roivainen, A.; Tolvanen, T.; Salomaki, S.; Lendvai, G.; Velikyan, I.; Numminen, P.; Valila, M.; Sipila, H.; Bergstrom, M.; Harkonen, P.; Lonnberg, H.; Langstom, B. *J. Nucl. Med.*, **2004**, *45*, 347.
[64] Lendvai, G.; Velikyan, I.; Bergstrom, M.; Estrada, S.; Laryea, D.; Valila, M.; Salomaki, S.; Langstom, B.; Roivainen, A. *Eur. J. Pharm. Sci.*, **2005**, *26*, 26.
[65] Kita, K.; Saito, S.; Morita, C. Y.; Watanabe, A. *Int. J. Cancer*, **1999**, *80*, 553.
[66] Sun, X.; Fang, H.; Li, X.; Rossin, R.; Welch, M. J.; Taylor, J. S. *Bioconjug. Chem.*, **2005**, *16*, 294.
[67] Morell, A. G.; Irvine, R. A.; Sternlieb, I.; Scheinberg, I. H.; Ashwell, G. *J. Biol. Chem.*, **1968**, *243*, 155.
[68] Halim, M.; Tremblay, M. S.; Jockusch, S.; Turro, N. J.; Sames, D. *J. Am. Chem. Soc.*, **2007**, *129*, 7704.
[69] Hanaoka, K.; Kikuchi, K.; Kobayashi, S.; Nagano, T. *J. Am. Chem. Soc.*, **2007**, *129*, 13502.

Received: March 08, 2008 **Revised: March 28, 2008** **Accepted: April 01, 2008**